Liquid-Liquid Transition Kinetics in D-mannitol

Chengrong Cao[1], Wei Tang[1], John H Perepezko[1*]

[1]Department of Materials Science and Engineering, University of Wisconsin-Madison, Madison, Wisconsin 53706, USA

*Corresponding author, perepezk@engr.wisc.edu

Abstract

The kinetics of the first order liquid–liquid transition (LLT) in a single-component liquid D-mannitol has been examined in detail by high rate of flash differential scanning calorimetry measurements (FDSC). By controlling the annealing temperature, the Phase X formation from supercooled liquid is distinguished by either a nucleation-growth or a spinodal-decomposition type of LLT. In the measured Time-Temperature-Transformation (TTT) curve the portion covering the nucleation-growth type of LLT can be well fitted with a Classical Nucleation Theory analysis.

Keywords: Polyamorphism, Liquid-liquid transition, transformation kinetics

Introduction

Polyamorphism characterizes the phenomenon where a substance can exist in two or more distinct amorphous states. The first report of polyamorphism was in water system by Mishima et al.[1] where it was demonstrated that water presented two amorphous phases with different densities at low temperature. Since this first report only a few elements[2-4], organic molecules[5,6] and inorganic systems[7] have been claimed as candidates for the polyamorphism. In prior work the first order polymorphic transformation has been established in D-mannitol [8-9]. In previous work[8] it was shown in the Time-Temperature-Transition (TTT) curve that the transformation boundary between Glass Normal (GN) and Phase X has the typical C curve shape. This together with the isothermal annealing heat flow plot indicates a thermally activated transformation. Considering the fact that GN and Phase X are two different amorphous states of D-mannitol, which means they have no composition

difference and no in-molecule structure difference, the transition from GN to Phase X should be understood as the change from one configuration to another. The Raman and NIR results from the Zhu et al. work[9,10] indicate that the GN and Phase X have different arrangements in hydrogen bonds. To understand the kinetic mechanism of the LLT and provide an analysis of the TTT curve, it is necessary to determine the detailed kinetics of the LLT.

In this work, new observations and analyses are provided on the transformation kinetics between the two amorphous states of D-mannitol. High rate differential scanning calorimetric measurements can precisely separate the behaviors of the two amorphous states and provide detailed energy evolution profile of the transformation. By using Flash DSC, two types of LLT, a nucleation-growth (NG)-type and a continuous spinodal-decomposition SD-type transformation are found and distinguished by isothermal and nonisothermal methods. The Classical Nucleation Theory (CNT) model has been utilized to provide a good account for the NG-type LLT.

Experimental methods

D-mannitol (Aldrich, > 99%) was used as received. The high rate DSC measurements were carried out on a Mettler Toledo Flash DSC2+, with allowed heating rates (β) ranging from 10 to 50000 K/s and cooling rates ranging from 10 to 10000 K/s. The samples used in the high-rate DSC measurements were selected from as received sample powder, with dimensions smaller than the DSC measurement chip sample area (60 x 60 μm^2) corresponding to a weight of about 200 ng with a volume of about 1.32 $\times 10^5$ μm^3. This sample size ensures reasonable signal/noise ratio and does not result in a signal delay. The weight of a sample can be calculated from its melting enthalpy in the Flash DSC heating trace and comparing the value to that for a bulk sample with known weight. Before measurements, the sample was heated to 10 K above its melting

point and held for 10 s to allow the development of good contact with DSC measurement chip. By choosing the Flash-DSC isothermal trace of the completely crystalline sample as a baseline that is subtracted from each of the annealing traces, the enthalpy changes under each annealing condition can then be calculated by integrating the heat flow rate. A typical Flash DSC measurement procedure is described in previous work[8] and the data acquired from last step in that procedure is used for providing information on the transformation kinetics.

Results:

In order to clarify the transformation behavior, a series of annealing treatments were conducted over the temperature, T_a range from 284 K (T_g of GN, T_gN) to 325 K. The thermal protocol is shown in Fig. 1a. When $T_a < 297$ K, the signal of exothermic peak is too weak for detection as shown for the isothermal trace at $T_a = 295$ K in Fig. 1b. For a $T_a \geqslant 297$ K, as shown in Fig. 1c for $T_a = 297$ K there is a broad exothermic peak during the LLT from supercooled liquid of GN (SCL-1) to Phase X (SCL-2). The integration of the heat release is also plotted versus annealing time t_a as the red dash curve in Fig. 1c. At the higher T_a the exothermic peak displays a stronger intensity in the annealing traces as illustrated in Fig. 1d for the isothermal annealing at $T_a = 310$ K. For $T_a > 322$ K, the crystallization becomes too rapid for the LLT peak to be distinguished clearly. The integrated enthalpy evolution for the above series of T_a is given in Fig.2. In all cases the enthalpy of the LLT shows that from 297 K to 317 K the enthalpy increases with T_a (30 J/g $\leqslant H_{max} \leqslant$ 66 J/g), while above 317 K it decreases with T_a.

The Johnson-Mehl-Avrami (JMA) equation can be applied to the enthalpy evolution:

$$x=1-exp(-Kt^n) \qquad (1)$$

In this equation, x is the degree of completion of the transition, K is the Avrami coefficient that represents the nucleation and growth characteristics of a transition, t is the time and n is the Avrami exponent. When the value of n varies from 1 to 4, it reflects the mechanism of the nucleation and the growth geometry. Calculated from

the isothermal traces of each T_a, the n values for the polyamorphic transition range from 3 to 4 for 297 K $\leqslant$ T_a $\leqslant$ 322 K indicating over all in this temperature range, SCL-1 to Phase X or supercooled liquid Phase X (SCL-2) is formed by a nucleation-growth type (NG-type) transition. From the isothermal annealing behavior shown in Fig.2 the onset time or delay time for the initiation of the LLT can be used to construct a TTT (time-temperature-transformation) diagram as presented in Fig. 3 which displays the typical C-curve shape that is characteristic for a nucleation and growth reaction.

Even though the LLT can be activated above T_gN[10], the isothermal measurements in the temperature range 284 K < T_a < 297 K did not detect a clear signal for the LLT. In order to investigate the characteristics of the LLT further a series of annealing treatments was conducted from 285 K to 310 K. Over this temperature range the characteristic time scale of the LLT ranges from a few to tens of seconds. In this series a 1000 K/s heating and cooling rate was employed to obtain a strong intensity signal in the FDSC.

For TPP, two types of LLTs[11-14] have been claimed depending upon different annealing conditions. A nucleation-growth type (NG-type) is induced by annealing at high T_a where on subsequent heating in the FDSC two separated T_g values are observed, where T_g does not change with the amount of the proceeding annealing. A spinodal-decomposition type (SD-type) is found by annealing at low T_a, where on subsequent heating, T_g continuously increases with increasing t_a.

For D-Mannitol, at the annealing temperature which lower than 300 K but above T_gN the onset of the glass transition is identified in the FDSC curves with various t_a as shown in Fig. 3a, where the marked points represent the onset of the glass transition. There is only one glass transition with an onset temperature that increases continuously and gradually from T_gN to T_gX (glass transition temperature of Phase X), which is the characteristic feature of a continuous or SD-type LLT[11]. At T_a = 285 K (T_gN +1 K), during heating the first endothermic peak of GN to SCL-1 grows with the increasing t_a ,

meanwhile following the first peak, for $t_a \geq 3000$ s the second small hump of SCL-2 to SCL-1 transition appears and then rises gradually as t_a increases as shown in Fig. 4a (the inserted thermal protocol is the typical FDSC measurement procedure of the forward SCL-1 to SCL-2 LLT process during annealing). At 285 K slightly above T_gN, the transformation from SCL-1 to Phase X is beginning to be activated and then after long time annealing the transformation amount increases with t_a, which is consistent with the conventional DSC, X-ray diffraction and near infrared spectroscopy results[10]. At a higher T_a = 290 K, Fig. 4b shows the second peak including the glass transition of Phase X to SCL-2 and then the LLT of SCL-2 to SCL-1 grows with t_a dramatically for $t_a > 100$ s and gradually merges to the second peak with the continuously increasing T_g. It is worth noting that the heat capacity (C_p) exhibits a minimum following the glass transition of GN, which is the reason for only one glass transition in the SD-type LLT[11]. The delay or onset time of the LLT decreases significantly with increasing temperature, so that as indicated in Fig. 4c, at T_a = 295 K the onset time (10 s < t_a < 40 s) for the initial second peak is much shorter than at the lower T_a.

When the LLT proceeds above 300 K, in Figs. 4d-f, T_gN is obtained before the completion of SCL-1 to Phase X so that the signal of GN to SCL-1 transition disappears completely upon sufficiently long annealing. At a high heating rate, T_gX is located around 327 K which is slightly above the stability limit of SCL-2 against SCL-1 upon heating[8], and the glass transition of Phase X to SCL-2 doesn't complete at this temperature within a short time. In other words, the Phase X to SCL-2 transition and SCL-2 to SCL-1 take place concurrently. Thus, it is difficult to separate them clearly. To quantify T_gX, it is identified by the onset of the second peak with the annealing time at about 10% of the relative enthalpy changes of the endothermic peak. In comparison with the SD-type LLT, for example, for T_a = 300 K, we identify T_gN ~ 300 K, T_gX ~ 327 K in Fig. 4d, indicating there are two distinct sequential transitions unambiguously. The first step is the GN to SCL-1 glass transition, the second one is including Phase X to SCL-2 glass transition and the reverse LLT from SCL-2 to SCL-1. The minimum of C_p following the first glass transition no longer appears which always exists in the SD-type LLT but never in the NG-type LLT. For TPP, the glass transition during NG-type

LLT stays almost constant as a function of t_a until the completion of the transformation. For D-Mannitol, the onset of T_gN shifts slightly with t_a until the first peak disappears, however, the variation range is less than 5 K which is significantly smaller than the variations in Figs. 4 a-c. In Fig. 3d, for T_a = 300 K, the onset of T_gX stays almost constant with t_a until the completion of LLT, while for the higher T_a as shown in Figs. 4e and 4f, due to the faster structural relaxation the onset of T_gX increases slightly with increasing t_a, and the variation tendency increases with T_a slightly as well.

As a summary all of the annealing results are plotted in Fig. 5. The trends indicate that for T_a $\leqslant$295 K for the SD-type LLT the onset of glass transition shifts gradually and continuously with t_a. However, for T_a $\geqslant$ 300 K the onset of T_gN and T_gX shift within a much smaller range and especially for T_a = 300 K, T_gX is almost constant for t_a < 300 s. Therefore, the critical temperature T_{SD}^{N-X} for the transition from the SD-type to NG-type forward LLT is located between 295 K with 300 K. This is consistent with the observation in conventional DSC quasi-static measurements that the exothermic peak position of the SCL-1 to Phase X transition is about 300 K[9,10].

To further verify the stability limit of SCL-2, the reverse LLT process for T_a = 300 K was performed following the experimental protocol shown in Fig. 6a. In this case the sample is kept for 0.1 s at T_{rc} before re-cooling from T_{rc}. The results in Fig. 6b show the re-cooling temperature T_{rc}-dependent second heating curves of reverse LLT for a sample annealed at 300 K for 500 s with completion of the LLT. With increasing T_{rc}, the endothermic peak becomes smaller and the signal intensity of GN to SCL-1 transition emerges and becomes stronger gradually. Because of the extremely short delay time of crystallization at a high temperature for $T_{rc} \geq$ 335 K, the onset temperature decreases gradually with an increase T_{rc}. The corresponding heat released during reverse LLT is shown in Fig. 6c. There is an inflection point for the decrease in the endothermic peak located around 325 K. Thus, this T_{rc} marks the stability limit of SCL-2 against SCL-1 upon heating, that is, the temperature above which SCL-2 becomes unstable against SCL-1. Therefore, the stability limit of SCL-2 is T_{SD}^{X-N} of 325 K, and

above T_{SD}^{X-N} the process takes place almost immediately without an incubation time, resulting in the reverse LLT taking place via a SD-type transformation. Although the T_gN doesn't shift from SCL-2 to SCL-1 as the SD-type transformation in Fig. 4a-c, the evolution of the onset temperature of T_gX increases continuously with the increase T_{rc} obviously when T_{rc} > 325 K as shown in Fig. 6b and 6c. In contrast, in the forward LLT process for T_a = 300 K, Fig. 6d shows the onset of T_gX stays almost constant before the completion of LLT for $t_a \leq 200$ s, and then for $t_a > 200$ s, it resumes a T_a dependence.

Discussion

Between the estimated T_{SD}^{N-X} and T_{SD}^{X-N} ranges (296, 325) K the forward LLT takes place by a NG-type transformation. Therefore, the CNT may be applied to fit the TTT curve. The homogeneous nucleation rate J can be expressed as [15,16]:

$$J = \rho_S Z \nu \, exp(-\frac{\Delta G^*}{kT}) \qquad (1)$$

Where ρ_s is the sample potential nucleation site density of $3\text{x}10^{14}$ m^{-3}, Z is the Zeldovich factor with a value of 0.01, ν is the atom attempt frequency that is represented by $\nu = \nu_0 \exp(-E/kT)$ with ν_0 a prefactor and, E is the barrier for atom attachment, ΔG^* is the nucleation barrier, k is Boltzmann's constant. When a nucleation event occurs within a volume V (volume of sample is about 1.32×10^5 μm^3), at a given temperature T, after an incubation time τ the onset of transition is defined by: $JVt = 1$. From this condition equation (1) can be expressed as:

$$ln(\tau) = C + \frac{E}{kT} + \frac{A}{T(T_L - T)^2} \qquad (2)$$

Where parameters $A = \frac{16\pi T_L^2 \sigma^3}{3k\Delta H^2}$ and $C = -ln(V\rho_S Z\beta_0)$.

The parameter σ represents the interfacial energy. ΔG_v is the driving free energy for nucleation, and can be calculated from: $\Delta G_v = \frac{\Delta H(T_L - T)}{T_L}$, with the value of the LLT enthalpy $\triangle H = 9.53\times10^7$ J/m^3[9]. T_L is the transition temperature between two amorphous states. Based on Terashima's interpretation[17] this temperature should be found from the plots of T_gX temperature against inverse heating rate, β^{-1} at infinite heating rate. To determine T_L the melt-quenched samples were annealed in the flash

DSC to fully transit into Phase X and the onset values of T_g were measured under different heating rates. The value of T_L is determined to be 346 K, as shown in Fig. 7a. Because the LLT is activated as the GN is supercooled into SCL-1, the activation energy of diffusion E can be related to the activation energy E of the structural relaxation in glass transition of GN. From the heating rate dependence of T_gN, E can be determined from [17]:

$$\frac{dln\beta}{d\left(\frac{1}{T_g}\right)} = -\frac{E}{k} \qquad (3)$$

The linear relationship between $ln\beta$ and $\frac{1}{T_g}$ plotted in Fig. 7b, gives $E = 2.1\pm0.04\times 10^5$ J/mol.

The TTT curve obtained from the isothermal measurements can be fitted with equation (2), as shown in Fig. 3 (red curve). Within the temperature range of the NG-type LLT the TTT curve can be nearly perfectly fitted with the following results: $A = \frac{16\pi T_L^2\sigma^3}{3k\Delta H^2} = 8.1 \pm 0.3 \times 10^6$ K^3. From the fitting results the values for $\frac{\Delta G^*}{kT}$ and r^*, can be determined using the following relations:

$$\frac{\Delta G*}{kT} = \frac{16\pi\sigma^3\cdot T_L^2}{3kT(T-T_L)^2\cdot\Delta H^2} \qquad (4)$$

$$r* = \frac{-2\sigma}{\Delta G_V} = \frac{-2\sigma\cdot T_L}{\Delta H(T_L-T)} \qquad (5)$$

Since the fitting is done on the isothermal measurement temperature range: (297, 322) K within the NG-type LLT range between T_{SD}^{N-X} = 296 K and T_{SD}^{X-N} = 325 K, the calculated $\frac{\Delta G^*}{kT}$ and r^*values have a range corresponding to the temperature range (297, 322) K. The calculated value for A gives the interfacial energy: $\sigma = 7.9 \pm 0.12\times10^{-3}$ J/m^2 and the calculation gives $\frac{\Delta G^*}{kT}$ in the range (9.7±0.3, 32.1±1.1) which is within the range where CNT is applicable [16] and r^*in the range (1.1, 2.1) nm. For polyalcohols the crystal/liquid interfacial energy is range from 0.01 to 0.03 J/m^2[19], which should be higher than the liquid /liquid or liquid/glass interfacial energy of D-mannitol. Therefore, the calculated $\sigma = 7.9\times10^{-3}$ J/m^2 is reasonable for the interfacial energy for the LLT. Furthermore, the small r^* indicates the critical size for starting the

polyamorphic transition in D-mannitol is only few molecules. The nucleation rate for the LLT can be evaluated from eq.1 based upon the range of ΔG*/kT values together with the relation between ν and the delay time, τ (ν =$(2Z\tau)^{-1}$ [16] as shown in Fig.8. As T_{SD} is approached the trend of J reveals increasing values that is related to the decrease in ΔG*/kT. The increase in J upon approaching T_{SD} has also been observed in TPP [20]. This behavior has been proposed to be due to the increase in fluctuations that can act to promote enhanced nucleation upon approaching $T_{SD.}$ [20-23].

Conclusion

This study has provided new evidence for the kinetics of the polyamorphic transformation in D-mannitol. To determine the mechanism of LLT in the supercooled liquid state in the temperature range between normal glass transition and crystallization (284, 330) K, Flash-DSC is employed with the methods of isothermal and nonisothermal measurements. At ambient pressure the transition temperature of SD-type to NG-type LLT for the forward SCL-1 to Phase X is determined as T_{SD}^{N-X}= 296 K, and the stability limit temperature of the SCL-2 to the SCL-1 transition is T_{SD}^{X-N} =325 K. Limited by these two stability temperatures, the TTT curve can be well fitted with CNT. The TTT curve implies the polyamorphic transition in D-mannitol is thermally activated. Beyond the region of the NG-type transformation the analysis of the TTT curve requires a consideration of other kinetic models.

Acknowledgements

We thank the NSF funded UW-Madison MRSEC DMR-1720415 for financial support and Professor Frans Spaepen for helpful comments.

References

[1] O. Mishima, L. Calvert, and E. Whalley, Nature **310**, 393 (1984).

[2] V. Brazhkin, R. Voloshin, S. Popova, and A. Umnov, Phys. Lett. A **154**, 413 (1991).

[3] Y. Katayama, T. Mizutani, W. Utsumi, O. Shimomura, M. Yamakata, and K.-i. Funakoshi, Nature **403**, 170 (2000).

[4] P. F. McMillan, M. Wilson, D. Daisenberger, and D. Machon, Nature Mater. **4**, 680 (2005).

[5] I. Cohen, A. Ha, X. Zhao, M. Lee, T. Fischer, M. J. Strouse, and D. Kivelson, The Journal of Physical Chemistry **100**, 8518 (1996).

[6] R. Kurita and H. Tanaka, Journal of Physics: Condensed Matter **17**, L293 (2005).

[7] S. Aasland and P. McMillan, Nature **369**, 633 (1994).

[8] W. Tang and J. Perepezko, J. Chem. Phys. **149**, 074505 (2018).

[9] M. Zhu, J.-Q. Wang, J. H. Perepezko, and L. Yu, J. Chem. Phys. **142**, 244504 (2015).

[10] M. Zhu and L. Yu, J. Chem. Phys. **146**, 244503 (2017).

[11] M. Kobayashi and H. Tanaka, Nat. Commun. **7**, 13438 (2016).

[12] H. Tanaka, R. Kurita, and H. Mataki, Phys. Rev. Lett. **92**, 025701 (2004).

[13] H. Tanaka, Phys. Rev. E **62**, 6968 (2000).

[14] R. Kurita and H. Tanaka, Phys. Rev. B **73**, 104202 (2006).

[15] J. H. Perepezko and K. Hildal, Philosophical Magazine **86**, 3681 (2006).

[16]] K.C. Russell, Advances in Colloid and Interface Science, **13**, 205 (1980).

[17] Y. Terashima, M. Tsuchie, K. Takeda, and M. Honda, Chem. Phys. Lett. **584**, 93 (2013).

[18] C. T. Moynihan, S. -K. Lee, M. Tatsumisago, and T.Minami, Thermochim. Acta. **280**, 153 (1996).

[19] C. Huang, Z. Chen, Y. Gui, C. Shi, G. G. Z. Zhang, and L. Yu, J. Chem. Phys. **149**, 054503 (2018).

[20] R. Kurita, H. Tanaka, Phys. Rev. B, **73**, 104202 (2006).

[21] V. Talanquer, D.W. Oxtoby, J. Chem. Phys. **109**, 223 (1998).

[22] P.R. ten Wolde, D. Frenkel, Science, **277**, 1975 (1997).

[23] R.P. Sear, J.. Chem. Phys., **114**, 3170 (2001).

Figure captions

Figure 1. The normalized isothermal annealing data and their integrations. **(a)** The Flash DSC method for the isothermal measurements. **(b)** The isothermal annealing trace at T_a =295 K. **(c)** The annealing time dependence of the heat flow rate at T_a = 297 K, the exothermic peak corresponds to the transition from SCL-1 to Phase X and the red dash curve is the corresponding integration. **(c)** The stronger intensity of transition signal in the annealing trace at T_a = 310 K and its integration.

Figure 2. The normalized heat flow integrations for the isothermal annealing traces at a series of T_a. The onset points of these integral curves represent the delay time for LLT.

Figure 3. The TTT curve plotted from the measured isothermal LLT onset within the limitations of two spinodal decomposition temperatures T_{SD}^{N-X} = 296 K and T_{SD}^{X-N}= 325 K. The NG-type LLT is well fitted by classical nucleation theory (red curve) with a R-square of 0.98.

Figure 4. The evolution of the reheating Flash DSC curve and glass transition during the processes of forward LLT. There are two steps of transition, the first step occurs around 300 to 320 K is the glass transition of GN to SCL-1, the following second step including the glass transition of Phase X to SCL-2 and then the reverse LLT of SCL-2 to SCL-1. **(a-c)** The annealing time t_a dependent evolution in SD-type LLT observed at annealing temperature T_a = 285 K, 290 K and 295 K. **(d-f)** The evolution in NG-type LLT observed at T_a = 300 K, 305 K and 310 K respectively.

Figure 5. Summary of the t_a dependent onset temperature of glass transition in the forward LLT process. The T_gX at slow heating rate is about 315 K drawn as a guide dash line to separate the T_gN and T_gX at high heating rate.

Figure 6. Reverse process of LLT and the behavior of glass transition. **(a)** Thermal protocol of reverse LLT. **(b)** Reverse process of LLT from SCL-2 to SCL-1, for the

sample annealed at T_a = 300 K for t_a = 500 s. **(c)** The re-cooling temperature T_{rc} dependence of the heat released upon heating for a sample annealed at 300 K for 500 s and the corresponding onset temperature of T_gX. **(d)** t_a dependence of the heat released by the reverse LLT upon heating for a sample annealed at 300 K and the corresponding onset temperature of T_gX.

Figure 7. The evolution of the glass transition versus heating rate βs. **(a)** Plots of T_gX and T_gN against β^{-1}. The data of T_gN against β^{-1} are presented as a comparison, to show that although Phase X is stronger than GN, its T_g doesn't shift significantly with increasing heating rate. The dash lines are given as a guide to the eyes. **(b)** Napierian Logarithm of heating rate β versus reciprocal of T_gN, and the red fitting line of slope.

Figure 8. The temperature dependence of the nucleation rate for the LLT in D-mannitol over the range for the nucleation and growth reaction.

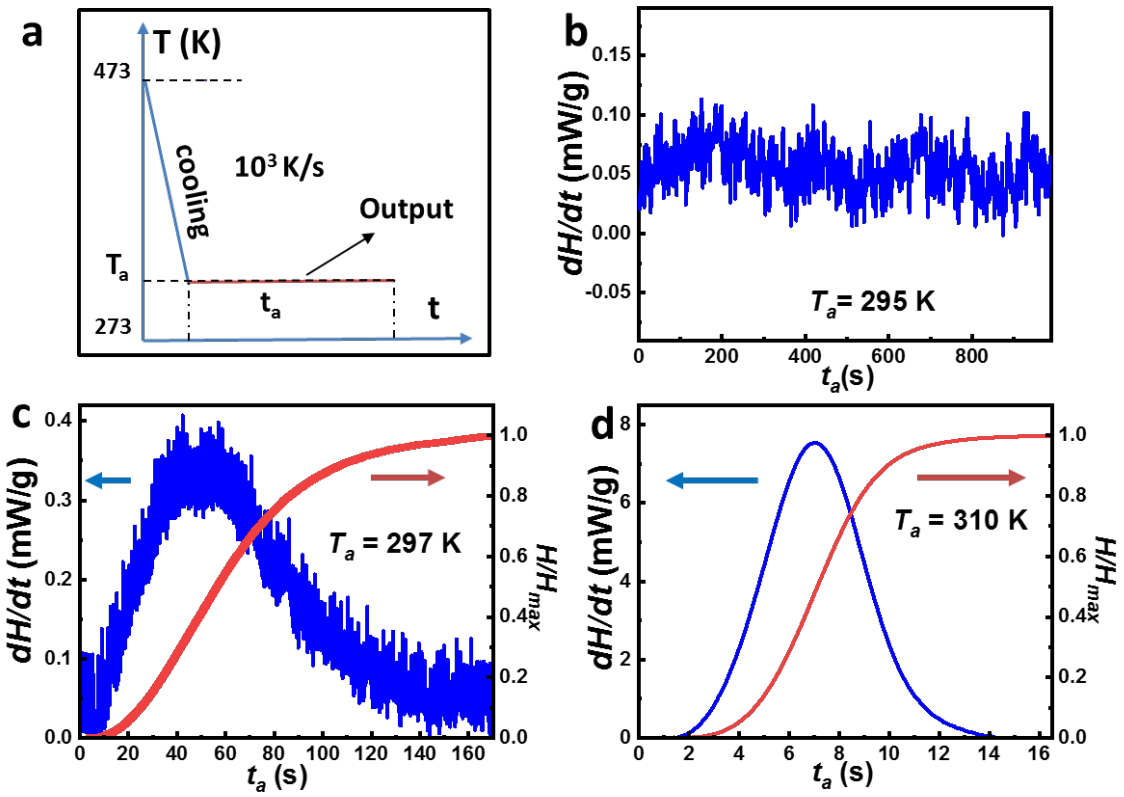

Figure 1. Cao, *et al.*

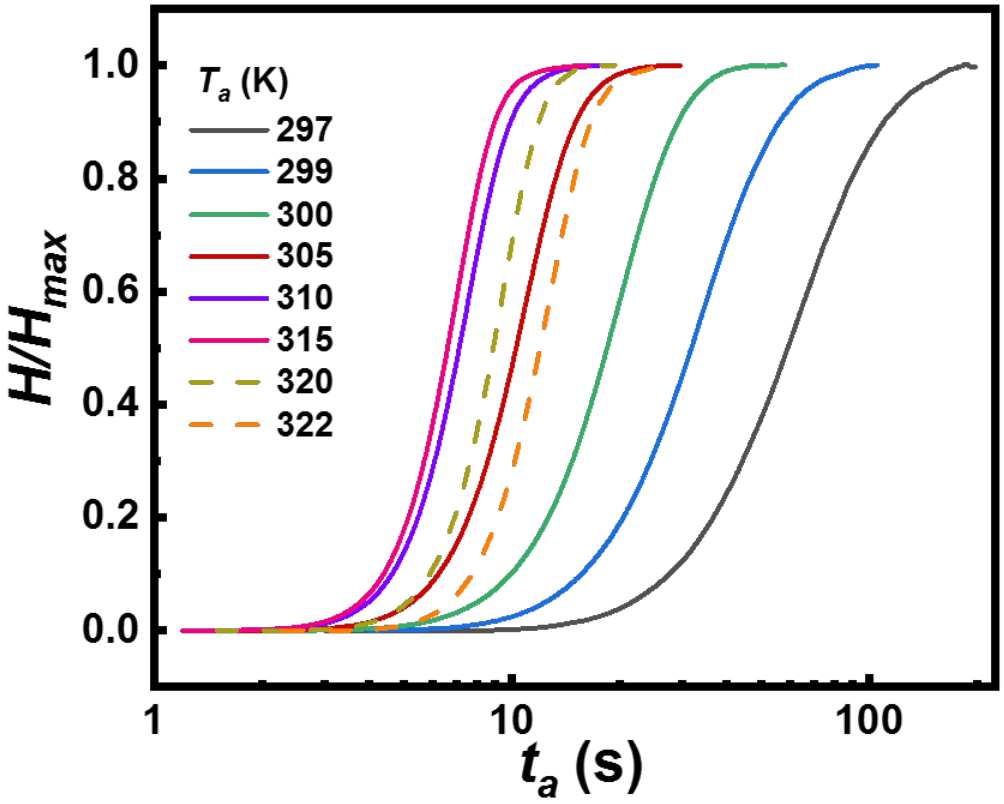

Figure 2. Cao, *et al.*

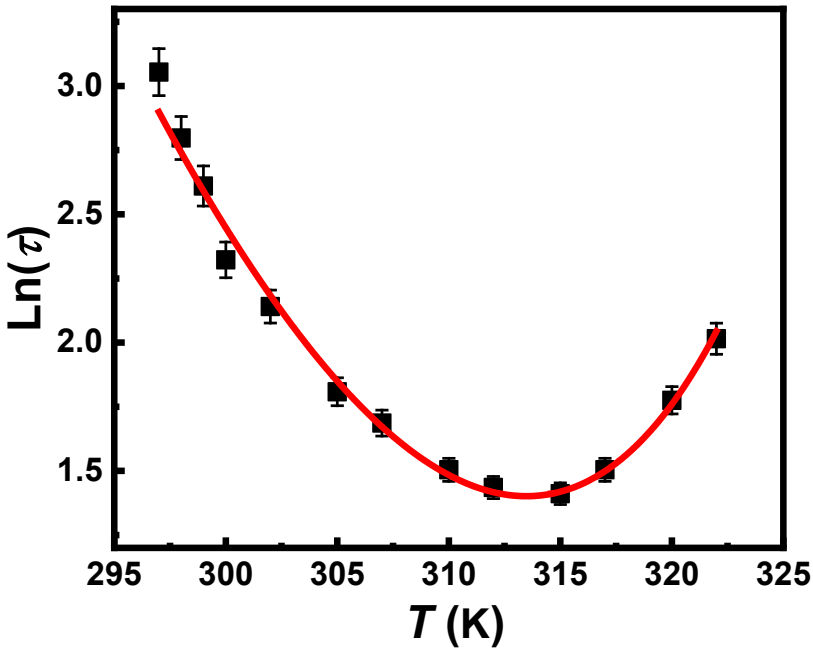

Figure 3. Cao, *et al.*

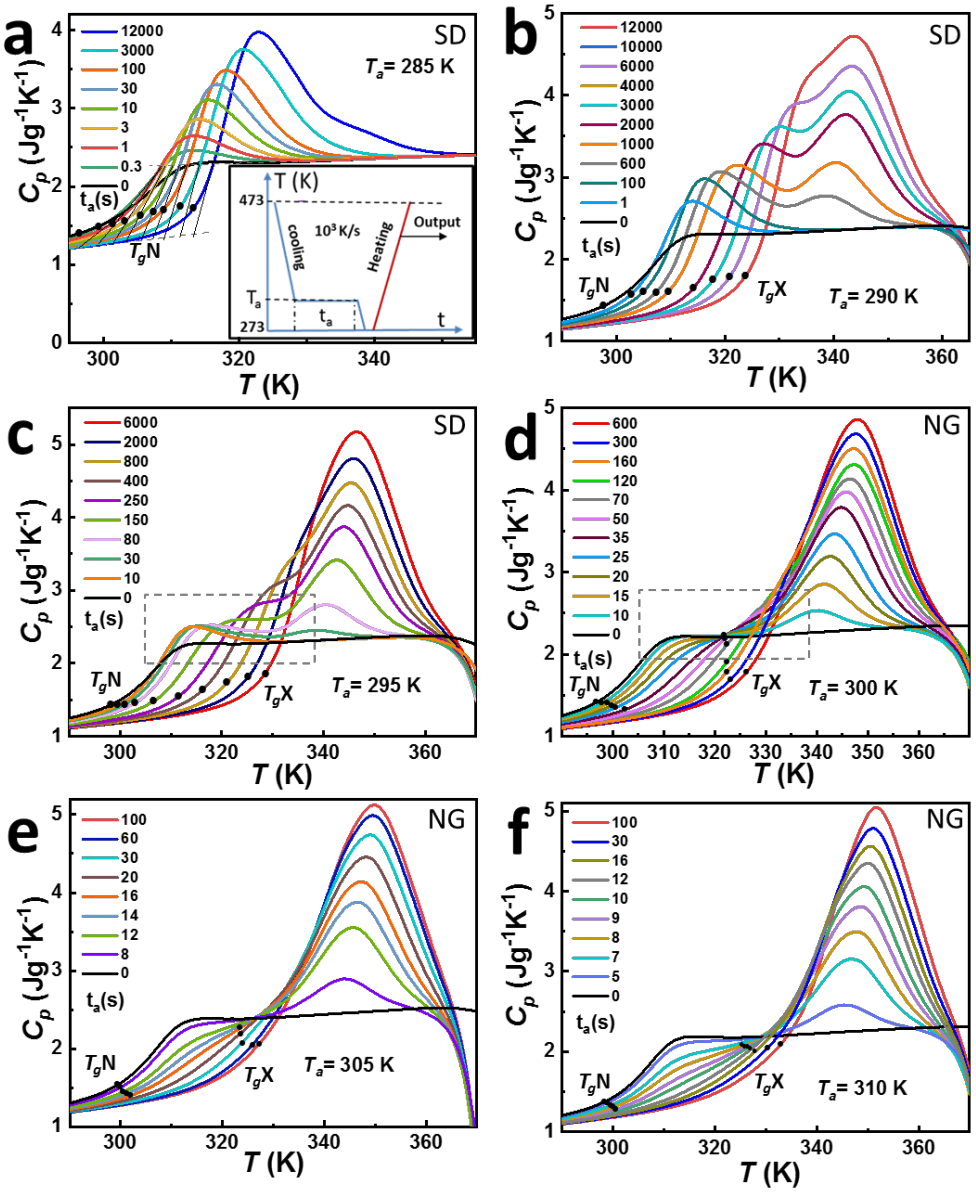

Figure 4. Cao, *et al.*

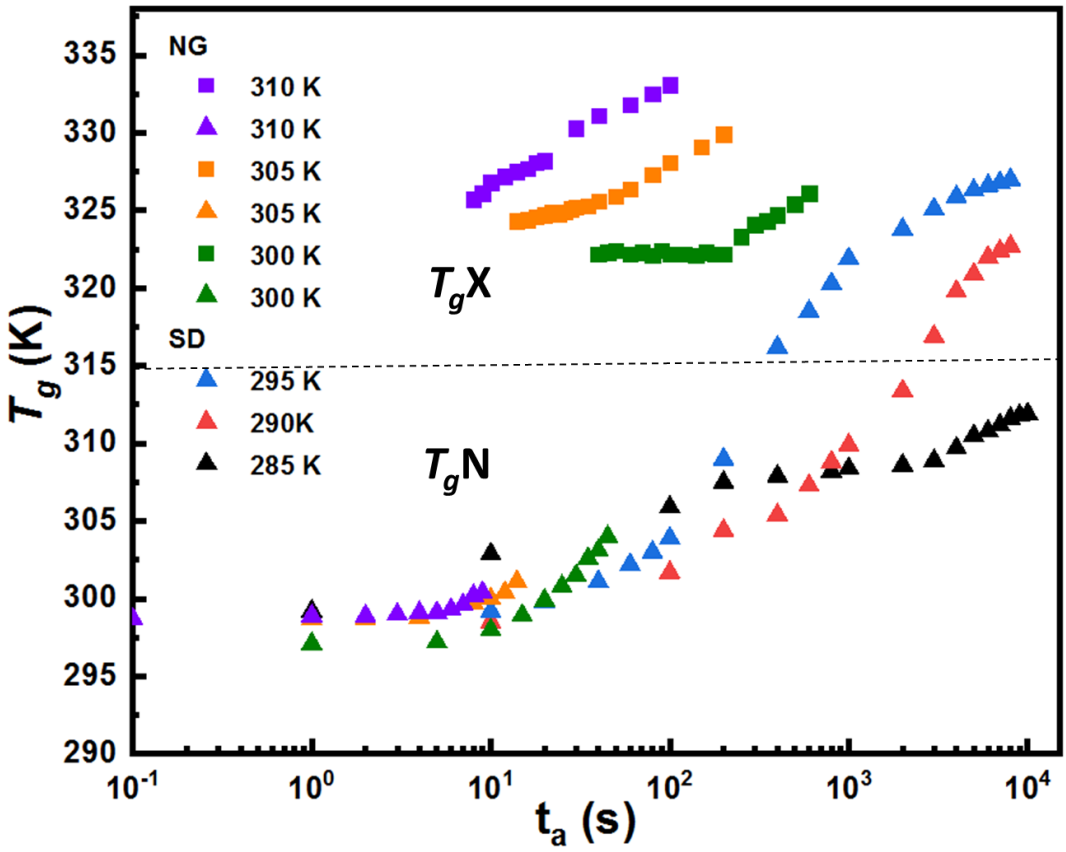

Figure 5. Cao,*et al.*

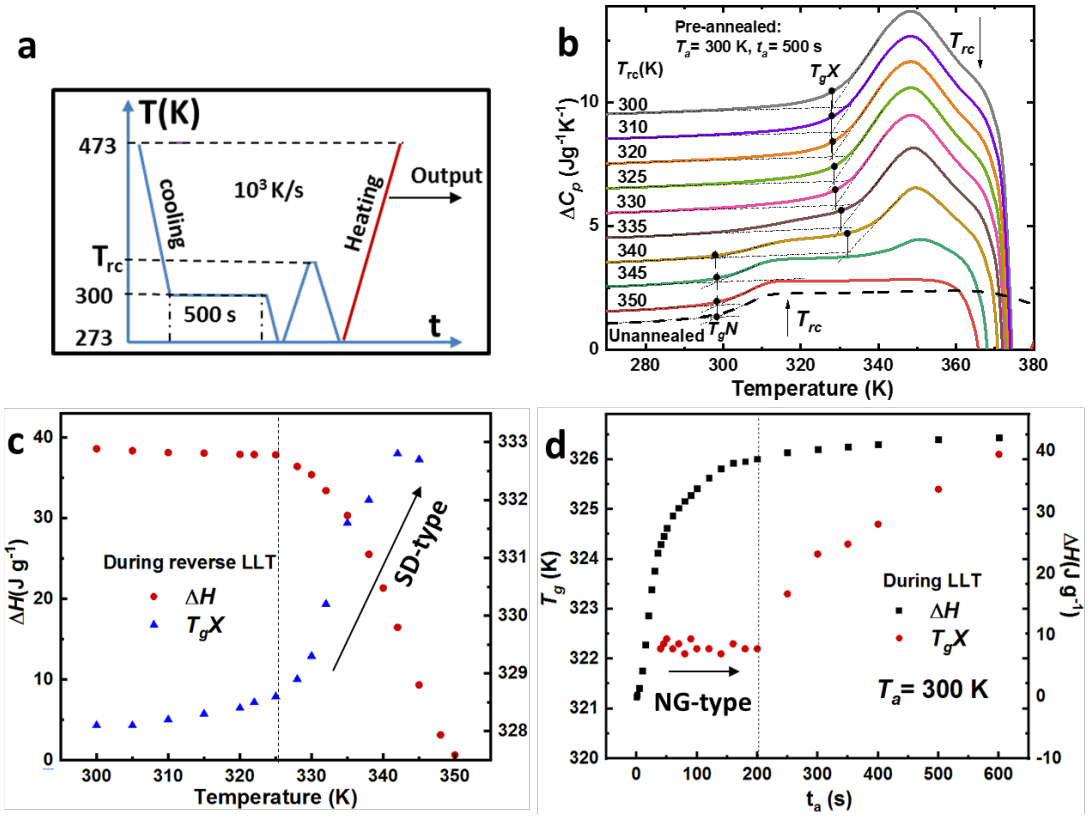

Figure 6. Cao, *et al.*

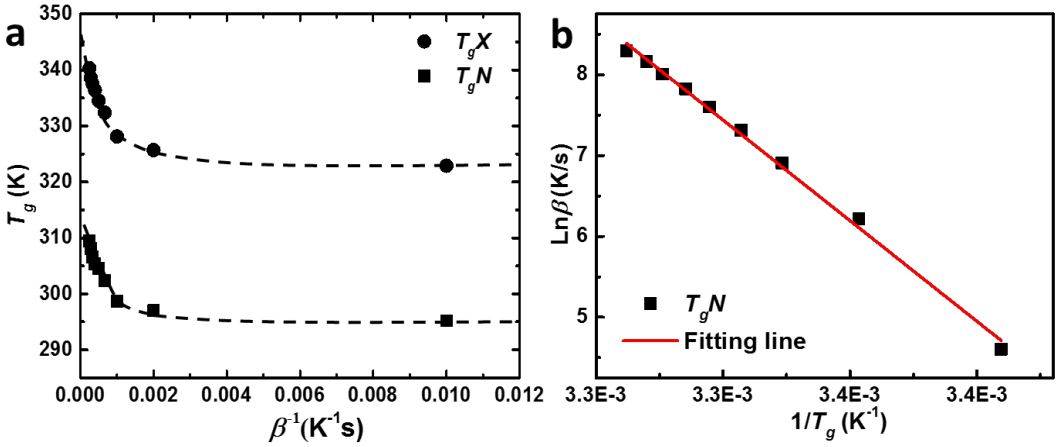

Figure 7. Cao, *et al.*

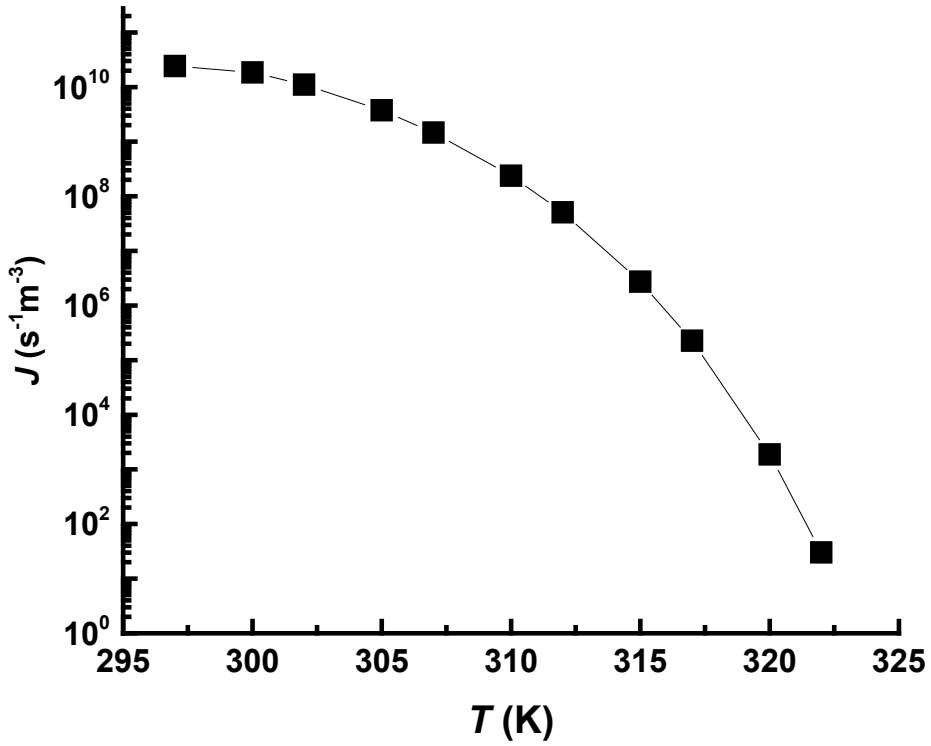

Figure 8. Cao, *et al.*